


Novel lymphoid enhancer-binding factor 1-cytoglobin axis promotes extravasation of osteosarcoma cells into the lungs

Mongkol Pongsuchart | Takahiro Kuchimaru | Sakiko Yonezawa |
Diem Thi Phuong Tran | Nguyen The Kha | Ngoc Thi Hong Hoang |
Tetsuya Kadonosono | Shinae Kizaka-Kondoh 

School of Life Science and Technology,
Tokyo Institute of Technology, Yokohama,
Japan

Correspondence: Shinae Kizaka-Kondoh,
School of Life Science and Technology,
Tokyo Institute of Technology, Yokohama,
Japan (skondoh@bio.titech.ac.jp).

Present address

Takahiro Kuchimaru, Center for Molecular
Medicine, Jichi Medical University 3311-1,
Yakushiji, Shimotsuke, Tochigi, Japan.

Funding information

This research was supported by a Grant-in-Aid for Scientific Research on Innovative Areas "Integrative Research on Cancer Microenvironment Network" from the Ministry of Education, Culture, Sports, Science and Technology of Japan (S.K.-K), Grant-in-Aid for Young Scientist (B) from Japan Society for the Promotion of Science (T.Ku), and Research Grants in the Natural Sciences (S.K.-K).

Lung metastasis is a major cause of mortality in patients with osteosarcoma (OS). A better understanding of the molecular mechanism of OS lung metastasis may facilitate development of new therapeutic strategies to prevent the metastasis. We have established high- and low-metastatic sublines (LM8-H and LM8-L, respectively) from Dunn OS cell line LM8 by using in vivo image-guided screening. Among the genes whose expression was significantly increased in LM8-H compared to LM8-L, the transcription factor lymphoid enhancer-binding factor 1 (LEF1) was identified as a factor that promotes LM8-H cell extravasation into the lungs. To identify downstream effectors of LEF1 that are involved in OS lung metastasis, 13 genes were selected based on LM8 microarray data and genomewide meta-analysis of a public database for OS patients. Among them, the cytoglobin (*Cygb*) gene was identified as a key effector in promoting OS extravasation into the lungs. *CYGB* overexpression increased the extravasation ability of LM8-L cells, whereas knocking out the *Cygb* gene in LM8-H cells reduced this ability. Our results showed a novel LEF1-CYGB axis in OS lung metastasis and may provide a new way of developing therapeutic strategies to prevent OS lung metastasis.

KEYWORDS

cytoglobin, extravasation, lung metastasis, lymphoid enhancer-binding factor 1, osteosarcoma

1 | INTRODUCTION

Osteosarcoma (OS) is the most common malignant bone tumor in both children and adults.^{1,2} Lung metastasis is a major cause of poor prognosis in OS patients. Although the 5-year survival rate of patients with localized disease is approximately 70%,^{3,4} that of patients with lung metastasis is less than 40%.⁴ Because no effective treatment is currently available to improve outcomes, the development of new therapeutic strategies based on the molecular mechanisms of OS lung metastasis is urgently required.

Metastasis is a multistep processes involving epithelial-mesenchymal transition (EMT), invasion, intravasation, circulation, extravasation, seeding, and outgrowth in secondary organs.^{5,6} Because many genes participate in each step, identification of a gene whose function is crucial for a particular step is important for developing a strategy to prevent metastasis. Extravasation occurs when cancer cells migrate to distant organs after entering the circulation. The process involves the adhesion of cancer cells to the endothelium, modulation of the endothelial barrier, and transmigration of cancer cells to reach the underlying tissue. First, adhesion between cancer cells and

This is an open access article under the terms of the Creative Commons Attribution-NonCommercial License, which permits use, distribution and reproduction in any medium, provided the original work is properly cited and is not used for commercial purposes.

© 2018 The Authors. *Cancer Science* published by John Wiley & Sons Australia, Ltd on behalf of Japanese Cancer Association.

vascular endothelial cells occurs through cell-adhesion molecules with ligand and receptor functions after cancer cell arrest in small capillaries.^{7,8} Then, secreted molecules from cancer cells induce alterations in the endothelial cell-cell junction architecture.⁸ In addition, cancer cells can interact with immune cells and platelets to induce cytokine production from those cells, facilitating the alterations.^{7,8} After endothelial barriers are disorganized, endothelial leakage and cancer cell transendothelial migration occurs. Identification of genes controlling OS extravasation may be able to prevent OS lung metastasis, but such genes have not been identified.

Wnt signaling and lymphoid enhancer-binding factor 1 (LEF1) advocate metastasis-promoting pathways in OS and other cancers.^{9–11} Inhibition of Wnt or silencing of *Lef1* expression significantly suppressed metastasis in vivo.^{9,10} LEF1, a member of the T-cell factor (TCF)/LEF family of high-mobility group transcription factors, is primarily involved in the canonical Wnt/ β -catenin signaling pathway.^{11,12} Although LEF1 is implicated in many steps of metastasis,¹¹ the underlying mechanism whereby LEF1 enhances lung metastasis in OS is still unclear.

Cytoglobin (CYGB) is a member of the globin family of proteins, which include hemoglobin and myoglobin.^{13,14} *Cygb* was first identified as an inflammatory- and fibrosis-related gene in the liver.¹⁵ In addition, *Cygb* is also known to function as a tumor suppressor gene^{16–18} and is involved in protective mechanisms against cellular stresses such as cell injury, DNA damage, and hypoxia.^{13,16,19–22} CYGB is induced by hypoxia-inducible factor-1 α (HIF-1 α), nuclear factor kappa-light-chain enhancer of activated B cells (NF- κ B), and other inflammation-related transcription factors.²³ Overexpression (OE) of CYGB in lung cancer cells impaired transmigration and anchorage-independent growth under normoxic conditions but promoted these abilities under hypoxic conditions.¹⁹ In the present study, we isolated LM8 sublines with differential abilities to metastasize to the lungs, and molecular genetic analyses of these sublines showed that LEF1-induced CYGB plays a crucial role in the extravasation step during lung metastasis. Our results indicate that a novel LEF1-CYGB axis can potentially serve as a therapeutic target for preventing the lung metastasis of OS.

2 | MATERIALS AND METHODS

2.1 | Cell culture

Murine OS LM8 cell line²⁴ was gifted by Dr Hideki Yoshikawa (Osaka University, Osaka, Japan). All LM8 sublines were cultured in DMEM supplemented with 5% FBS, penicillin (100 U/mL), and streptomycin (100 μ g/mL at 37°C, 5% CO₂). Murine vascular endothelia bEnd.3 cells were purchased from the ATCC (Manassas, VA, USA). bEnd.3 cells were cultured in DMEM supplemented with 10% FBS, penicillin (100 U/mL), and streptomycin (100 μ g/mL) at 37°C, 5% CO₂.

2.2 | Mice

Male BALB/c nu/nu, SCID, and C3H mice were obtained from Charles River Laboratory, Japan (Yokohama, Japan). All mice used

were 6–8 weeks of age and were housed in the animal facilities at Tokyo Institute of Technology. All experimental procedures involving mice were approved by the Animal Experiment Committees of Tokyo Institute of Technology (authorization numbers 2010006 and 2014005) and carried out in accordance with relevant national and international guidelines.

2.3 | In vivo and ex vivo bioluminescence imaging

Bioluminescence (BL) images of mice were acquired using the IVIS[®] Spectrum system (PerkinElmer, Waltham, MA, USA) 15 minutes after i.p. injection with D-luciferin (50 mg/kg) (Promega, Madison, WI, USA). Ex vivo imaging was immediately carried out after the last in vivo image was taken. The following conditions were used for image acquisition: open emission filter, exposure time = 60 seconds, binning = medium 8, field of view = 12.9 \times 12.9 cm, and f/stop = 1. BL images were analyzed using Living Image 4.3 software (PerkinElmer).

2.4 | Establishment of LM8-L and LM8-H

The LM8/luc cell line was established by stable transfection with a firefly luciferase gene as described previously.²⁵ To establish LM8-L cells, which have lost the ability to metastasize to the lungs, LM8/luc cells were intracardially injected into BALB/c nude mice, and LM8/luc cells that metastasized to the bone were isolated with a BL image-guided approach. The isolated cells were cultured and reinjected into nude mice. LM8-L was established after 4 rounds of the image-guided in vivo screening process. LM8-H was selected based on metastatic ability to the lung in C3H mice from LM8-L sublines that were isolated from lung metastases generated after injection of LM8-L into the tibia of SCID mice.

2.5 | Lung metastasis assay

C3H mice were i.v. injected with LM8 sublines (10⁶ cells/100 μ L PBS: 137 mmol/L NaCl; 2.7 mmol/L KCl; 4.3 mmol/L Na₂HPO₄; 1.47 mmol/L KH₂PO₄). BL signals from the lungs were monitored through in vivo BL imaging on indicated days.

2.6 | Histology analysis

Isolated lungs were embedded in optimal cutting temperature (OCT) compound (Sakura Fine Tech, Tokyo, Japan) and stored at –80°C. Fixed lung cryosections of the lung (10- μ m thick) were then stained with HE.

2.7 | Tumor formation ability assay

For s.c. transplantation, cell suspensions (10⁶/20 μ L PBS) were mixed with 20 μ L Geltrex[®] (Thermo Fisher Scientific, Waltham, MA, USA) after which the mixture was s.c. injected into the hind limb of mice anesthetized with pentobarbital sodium (Somnopenyl; Kyoritsu

Seiyaku Corp., Tokyo, Japan). Thirty days after transplantation, tumors were excised and their weights were measured.

2.8 | Western blotting

Cell lysates were prepared with RIPA buffer and subjected to western blot analysis using a rabbit anti-LEF1 polyclonal antibody (Ab; Cell Signaling Technology, Danvers, MA, USA), a rabbit anti-CYGB polyclonal Ab (Thermo Fisher Scientific), and a mouse anti- β -actin monoclonal Ab (Sigma Aldrich, St Louis, MO, USA).

2.9 | Cell-proliferation assay

Cell proliferation was evaluated with the water-soluble tetrazolium salt 1 (WST-1) reagent (Roche Diagnostics, Basel, Switzerland) according to the manufacturer's instructions. Briefly, cells (10^3 cells/100 μ L culture medium) were seeded in a 96-well plate. After culturing for 24, 48, or 72 hours, the medium was removed and 100 μ L WST-1 (10-fold dilution with culture medium) was added to each well. The cells were further incubated for 3 hours and, then, the absorbance of each well was measured at 450 nm with a reference wavelength of 750 nm, after shaking the plate for 1 minute with a 680XR microplate reader Model (Bio-Rad, Hercules, CA, USA).

2.10 | Extravasation assay

Cells were labeled with 25 μ mol/L CellTracker[®] Green and i.v. injected into C3H mice (10^6 cells/100 μ L PBS). DyLight[®] 594-labeled isolectin B4 (6 mg/kg) (Vector Laboratories, Burlingame, CA, USA) was i.v. injected to stain endothelial cells 5 minutes before dissecting mice. The lungs were removed and observed under a confocal fluorescence microscope (Carl Zeiss, Jena, Germany) 48 hours after LM8 injection. Average fluorescence intensity of 3 fields/sample was quantitatively analyzed using ImageJ software.²⁶

2.11 | Cell-adhesion assay

bEnd.3 cells were seeded on a 24-well plate (10^5 cells/well) and cultured for 3 days. LM8 sublines were labeled with 25 μ mol/L CellTracker[®] Green for 30 minutes. After washing with PBS, LM8 cells (5×10^4) were seeded into 24-well plates with bEnd3 monolayers. After a 1-hour incubation, each well was washed 3 times with PBS. Number of LM8 cells attached to the bEnd3 monolayer was observed by fluorescence microscopy (4 fields/well) and quantitatively analyzed using ImageJ software.²⁶ Each sample was analyzed in triplicate.

2.12 | Transmigration assay

bEnd.3 cells (10^5) were seeded in the top filters with 8- μ m-pore Transwell[®] plate (Corning, Corning, NY, USA) and grown for 3 days. LM8 sublines were labeled with 25 μ mol/L CellTracker[®] Green for 30 minutes. After washing with PBS, the cells (5×10^4) were seeded

on bEnd.3 monolayers. After a 24-hour incubation, the unmigrated cells were wiped off with a cotton swab and, then, the filter was fixed with 4% paraformaldehyde for 20 minutes. The migrated cells on the filter were then observed under a fluorescence microscope (4 fields/filter) and the number of migrated cells was analyzed using ImageJ software.²⁶ Results are shown as the average number of cells per field. Each sample was analyzed in triplicate.

2.13 | Genomewide meta-analysis

Microarray data sets were downloaded from the public Gene Expression Omnibus (GEO) repository (<http://www.ncbi.nlm.nih.gov/gds>). The first data set included low- and high-metastatic clinical OS samples (GSE21257). The second data set included low- and high-metastatic human OS cell lines (GSE49003). The genes commonly upregulated in highly metastatic OS in both data sets were analyzed using GEO2R (<https://www.ncbi.nlm.nih.gov/gds>), and genes whose *P*-values were $<.05$ were selected. Gene IDs of selected human genes were converted to murine gene IDs using BioMart web software.²⁷

2.14 | Reverse transcription-PCR and qPCR

Total RNA was extracted from cell pellets using the RNeasy[®] Mini Kit (Qiagen, Valencia, CA, USA), as recommended by the manufacturer. Total RNA (1 μ g) was reverse-transcribed with Oligo(dT)20 Primer (Toyobo Co., Osaka, Japan) and ReverTra Ace (Toyobo Co.). qPCR and RT-PCR were carried out using Thunderbird[®] SYBR qPCR Mix (Toyobo) and EmeraldAmp[®] GT PCR Master Mix (Takara, Tokyo, Japan), respectively. The primer sets used for qPCR and RT-PCR are shown in Table S1.

2.15 | Gene KO using the CRISPR-Cas9 system

Two guide RNAs (gRNA1 and gRNA2) used for editing *Lef1* and *Cygb* were constructed using CRISPR design software.²⁸ The sequences of gRNA1 and gRNA2 used for targeting *Lef1* are 5'-TTGTTGTA-CAGGCCTCCGTC-3' and 5'-GTACGGGTCGCTGTTCATAT-3', respectively. The sequences of gRNA1 and gRNA2 used for targeting *Cygb* are 5'-GAAGGCGGTTTCAGGCTACGT-3' and 5'-TGAAG-TACTGCTTGCCGAA-3', respectively. The *Lef1* and *Cygb* gRNAs were inserted into a unique *BbsI* site of the pX330 plasmid (42230; Addgene, Cambridge, MA, USA). We used a fluorescence indicator system using the pCAG/EGFP plasmid²⁹ provided by Dr Ikawa (Osaka University, Osaka, Japan) to select cells whose genomes were correctly edited using the CRISPR-Cas9 system. GFP-positive colonies were selected, and 2 independent LM8-H/*Lef1*-KO and LM8-H/*Cygb*-KO clones each were established from the gRNA1- and gRNA2-mediated KO cells.

2.16 | Vector construction

The coding sequence of *Cygb* (NM_030206) was amplified using the KOD[®] FX Kit (Toyobo) with the following primer set: forward, 5'-

TCATGGAGAAA-GTGCCGGGCG-3' and reverse, 5'-CCCAAAGTGCTGCCAGGGAGG-3'. The PCR product was purified by Gelase® (Epicentre, Madison, WI, USA) and ligated into an *EcoRV*-digested pcDNA3.1-myc-His plasmid (Invitrogen, Carlsbad, CA, USA) using the Quick Ligation Kit (New England BioLabs, Cambridge, MA, USA) to construct the pcDNA3.1/*Cygb*. The pT2-MCS-SVNeo vector containing multicloning sites (MCS) was constructed using the pT2-SVNeo vector (26553; Addgene), as described previously.³⁰ The fragment containing the *Cygb* coding sequence was obtained by digesting pcDNA3.1/*Cygb* with *EcoRI* and *NotI* and inserting the liberated fragment into an *EcoRI*- and *NotI*-digested pT2-MCS-SVNeo plasmid.

2.17 | Establishment of an LM8 cell line with stable *CYGB* overexpression

To establish stable cell lines overexpressing *Cygb*, the sleeping beauty transposon system was used.³⁰⁻³² The pT2/*Cygb* or pT2-MCS-SV Neo and pCMV(CAT)T7-SB100 plasmids (34879; Addgene) were cotransfected into LM8-L cells using an electroporator (Nepa Gene, Chiba, Japan) according to the manufacturer's instructions. After 48 hours, the culture medium was changed to selection medium containing 1 µg/mL G418 (Roche Life Sciences). The cells were further cultured in selection medium for 14 days, and single colonies were isolated to establish *CYGB*-overexpressing LM8-L (*CYGB*-OE) cells.

2.18 | Statistical analysis

Data are presented as the mean ± SE and were statistically analyzed with a 2-sided Student's *t* test. *P*-values <.05 were considered statistically significant.

3 | RESULTS

3.1 | Establishment of murine OS sublines with differential lung-metastatic abilities

The LM8/luc cell line was previously established²⁵ by stable transfection with a constitutive firefly luciferase reporter gene in the highly lung-metastatic murine OS cell line, LM8.²⁴ LM8-L cells, with a low lung-metastatic ability, were established after 4 rounds of image-guided *in vivo* screening of LM8/luc cells, and LM8-H cells, with a high lung-metastatic ability, were isolated from cells in the LM8-L subline that regained lung-metastatic ability (Figure S1). Although LM8-L and LM8-H showed different cellular morphologies (Figure 1A), the expression levels of genes related to EMT therein did not show typical expression patterns of epithelial or mesenchymal cells (Table S2). Their differential lung-metastatic abilities were confirmed by *in vivo* injection into syngeneic C3H mice: significantly higher BL signals were observed in the lungs of mice injected with LM8-H cells compared to mice injected with LM8-L (Figure 1B). Histological analysis of the lungs further confirmed the higher lung-metastatic ability of LM8-H cells (Figure 1C). However, the *in vitro* proliferation rate of LM8-H cells was significantly lower than that of LM8-L cells (Figure S2), and the growth of *s.c.* LM8-H tumors was significantly slower than that of *s.c.* LM8-L tumors (Figure 1D). These results are consistent with the previous reports^{33,34} and suggest that the larger metastatic foci observed with LM8-H cells were not as a result of its higher degree of outgrowth in the lungs.

3.2 | Lymphoid enhancer-binding factor 1 regulated OS lung metastasis

To identify genes responsible for their differential lung-metastatic abilities of LM8-L and LM8-H cells, their gene-expression profiles

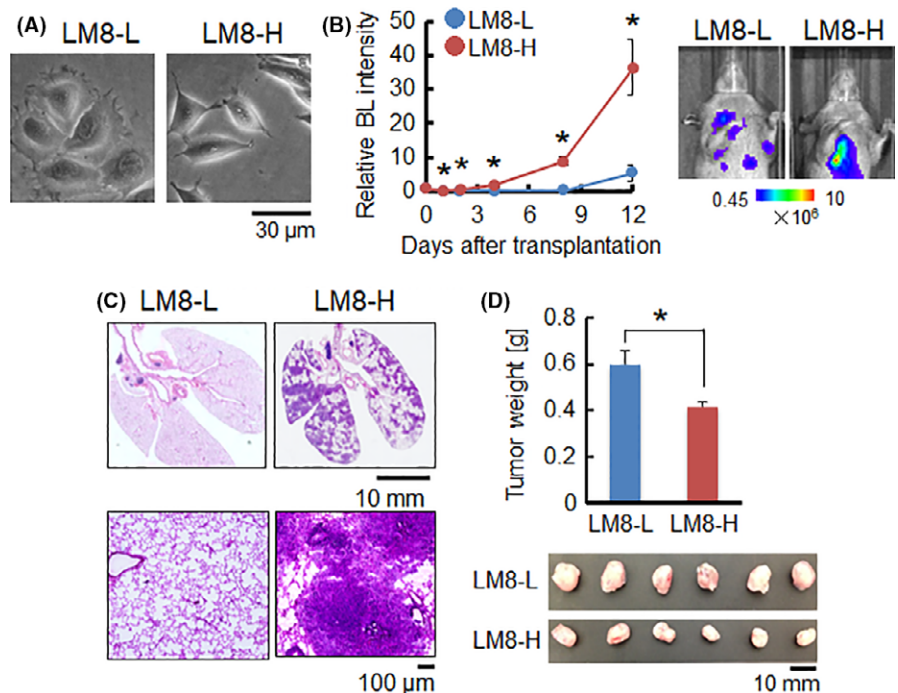


FIGURE 1 LM8 cells with different lung-metastatic potential. A, Microphotographs of the high-metastatic (LM8-H) and low-metastatic (LM8-L) cells. B, Lung-metastatic abilities of LM8-L and LM8-H cells. Representative *in vivo* bioluminescence (BL) images on day 12 (left) and quantitative analysis (right) are shown. BL signals from the lungs were normalized to those on day 0. *n* = 5, **P* < .05. C, Representative HE-stained images of lung tissues at 14 days after injection of the indicated LM8 sublines. D, Subcutaneous tumor formation. LM8 sublines were injected *s.c.* into C3H mice. Tumors were excised on day 30 (bottom photos). Their weights were measured, and average values are shown. *n* = 6. **P* < .05

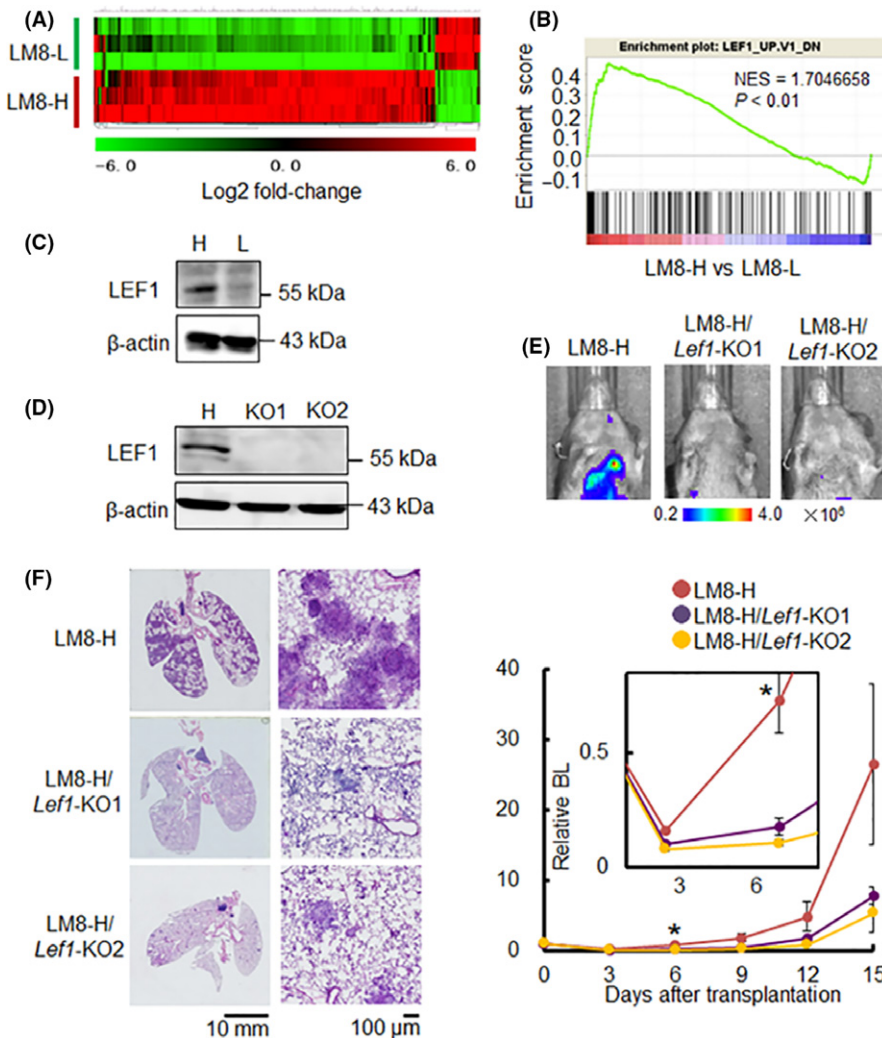


FIGURE 2 Lymphoid enhancer-binding factor 1 (LEF1) expression level correlated with the lung-metastatic potential of LM8 cells. A, Heat map analysis of microarray data of LM8 sublines. The heat map shows 500 genes with the greatest differential expression (fold-change >2) between the LM8-H and LM8-L cells. B, Gene set-enrichment analysis of *Lef1* in the LM8 sublines. C, LEF1 protein-expression levels in LM8-H (H) and LM8-L (L) cells. D, Establishment of *Lef1*-KO sublines from LM8-H (H) cells. LEF1 expression in LM8-H/*Lef1*-KO1 (KO1) and LM8-H/*Lef1*-KO2 (KO2) cells was examined by western blotting. E, Lung-metastatic ability of the LM8-H and LM8-H/*Lef1*-KO sublines. Representative in vivo bioluminescence images on day 15 (top) and quantitative analysis of BL signals (bottom) are shown. The inset graph shows an enlarged view from days 3 and 6. BL signals from the lungs were normalized by those on day 0. $n = 3$, $*P < .05$ (LM8-H vs LM8-H/*Lef1*-KO1 or LM8-H/*Lef1*-KO2 cells). F, Representative HE staining of the lungs at 15 days after i.v. injection of the LM8 sublines

were obtained through DNA microarray analysis (Figure 2A). Gene set-enrichment analysis showed that genes associated with LEF1 and several pathways such as AKT and MAPK were enriched in LM8-H cells (Figure 2B; Table S3). Among them, LEF1-related genes were prominent and highly expressed in LM8-H. Differential LEF1 protein-expression levels in these LM8 sublines were confirmed by western blotting (Figure 2C). To examine the significance of LEF1 expression in lung-metastatic ability of LM8-H cells, *Lef1* KO cell lines were generated using the clustered regularly interspaced short palindromic repeats (CRISPR)-CRISPR-associated protein 9 (Cas9) system, and 2 independent *Lef1* KO clones (LM8-H/*Lef1*-KO1 and LM8-H/*Lef1*-KO2) were established using different gRNA (Figure 2D). When the *Lef1* KO clones were i.v. injected into C3H mice, it was found that KO of *Lef1* significantly suppressed the lung metastasis of LM8-H cells (Figure 2E,F).

3.3 | Lymphoid enhancer-binding factor 1 regulated the extravasation step of LM8 sublines

Considering that the results described thus far were obtained using i.v. injection of LM8 sublines, promotion of metastasis by LEF1 observed in LM8-H cells occurred at the step after the cells enter the circulation. To identify the step in which LEF1 plays a crucial role

in LM8-H, we first observed lung tissues at 48 hours after tail vein injection with LM8 sublines by fluorescent confocal microscopy. Strikingly, LM8-H cells successfully extravasated into the lung parenchyma and proliferated, whereas all LM8-L and LM8-H/*Lef1*-KO cells remained in the blood vessels (Figure 3A; Figure S3), suggesting that LEF1 functions in the extravasation step. To assess the extravasation abilities, which are the abilities of the LM8 sublines in vitro to adhere to and transmigrate through the blood vessels (adhesion and transmigration abilities), adhesion and transmigration assays were carried out with cultured monolayers of murine endothelial cells. Consistent with the observations in lung tissues, LM8-L and LM8-H/*Lef1*-KO1 cells showed significantly reduced adhesion and transmigration abilities compared to LM8-H cells (Figure 3B,C). These results strongly suggest that the extravasation step could be responsible for differential lung metastasis abilities of LM8-L and LM8-H cells and that LEF1 function is indispensable in the extravasation of LM8-H cells to the lungs.

3.4 | Identification of CYGB as a downstream effector of LEF1

Lymphoid enhancer-binding factor 1 is a well-known transcriptional factor that mediates nuclear responses to Wnt signaling.¹¹ To

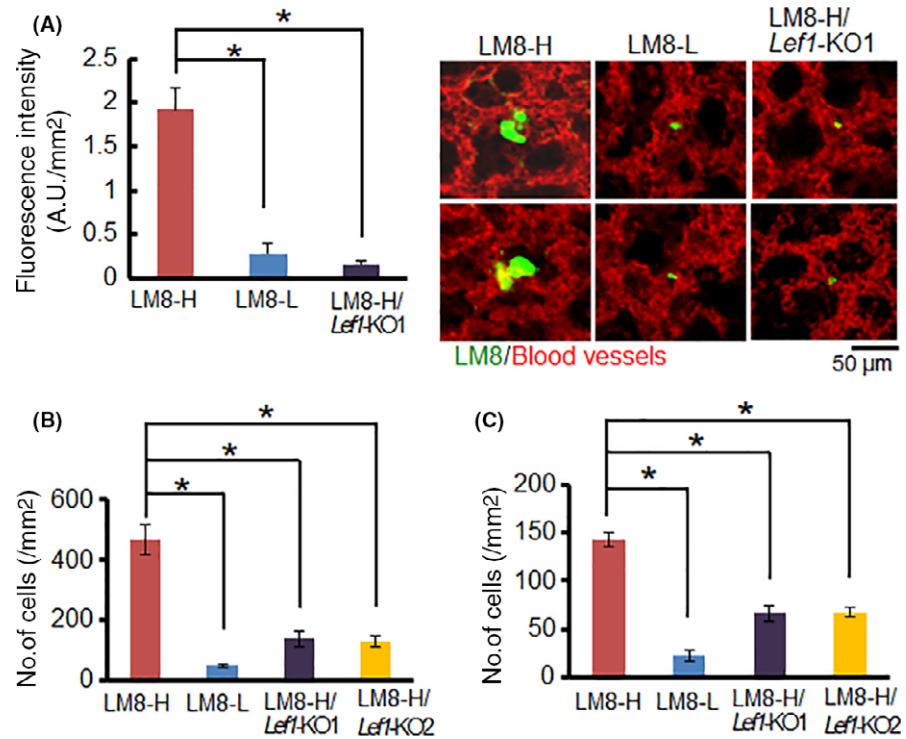


FIGURE 3 Extravasation abilities of LM8 sublines. A, Quantitative analysis (left) and representative images (right) of the lung 48 h after i.v. injection of the green-fluorescently labeled LM8 sublines. Endothelial cells stained red. n = 9, *P < .05. B, Adhesion abilities. Number of fluorescently labeled cells (LM8 sublines) attached to the endothelial monolayer was counted. n = 3, *P < .05. C, Transmigration ability. Number of fluorescently labeled cells that migrated through the vascular endothelial monolayer was counted. n = 3, *P < .05

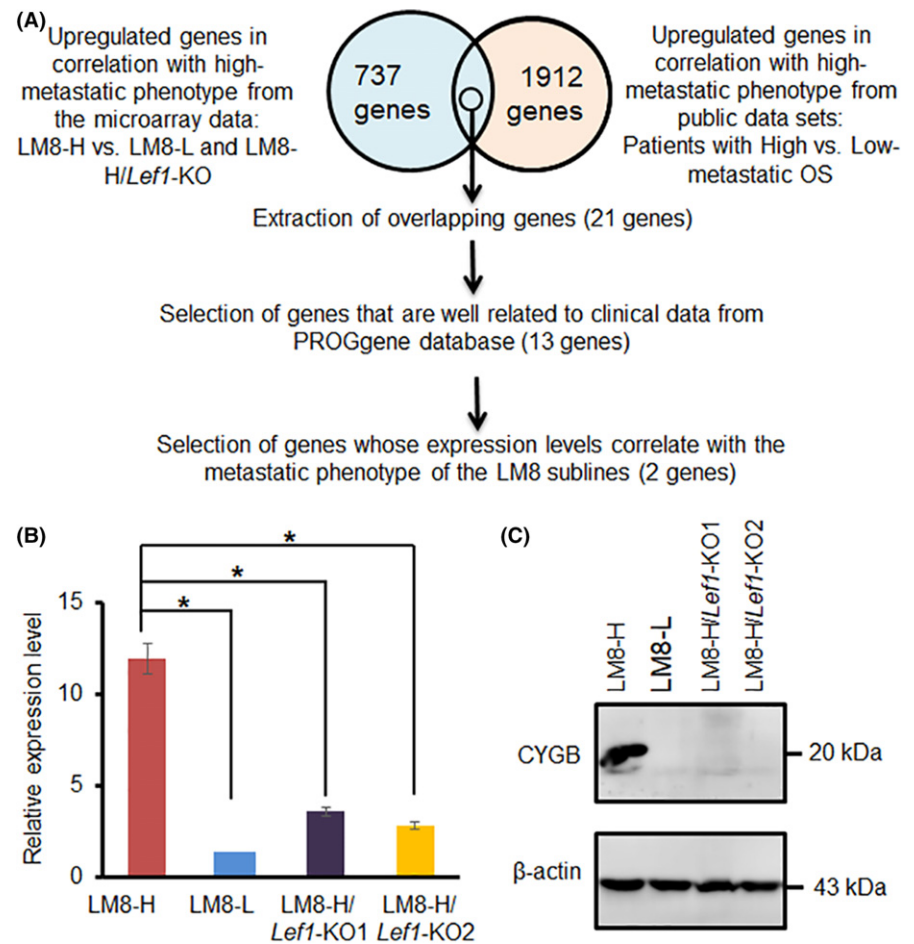


FIGURE 4 Identification of CYGB as downstream effectors of lymphoid enhancer-binding factor 1 (LEF1). A, Diagram of the process used to narrow down candidate genes by genomewide meta-analysis. Number of genes indicated for each step is the number of selected genes. B, Relative *Cygb* mRNA expression levels in the LM8 sublines to LM8-L analyzed by qRT-PCR. C, Protein-expression levels of CYGB in the LM8 sublines. CYGB, cytoglobin; OS, osteosarcoma

identify genes that are regulated by LEF1 and are responsible for the differential extravasation abilities among the LM8 sublines, pro-metastatic genes downstream of *Lef1* were first selected by genome-wide meta-analysis and DNA microarray data for the LM8 sublines (Figure 4A). By carrying out genomewide meta-analysis with public data sets for human OS cells, 1912 genes were selected as upregulated genes detected in patients with highly metastatic OS. From the DNA microarray data for the LM8-L, LM8-H, and LM8-H/*Lef1*-KO sublines, 737 genes were selected as upregulated genes in correlation with the metastatic phenotype of the LM8 sublines. The genes selected by the genomewide meta-analysis and the DNA microarray data were compared and 21 overlapping genes were extracted. Then, 13 out of 21 genes were selected based on their correlation with patient prognosis using the PROGgene database³⁵ (Table S4; Figure S4). Expression levels of the 13 candidate genes were analyzed by RT-PCR to examine their correlations with the metastatic phenotype of the LM8 sublines (Figure S5). Among them, the expression levels of *Cygb* and *Ddx58* were well correlated with the metastatic phenotype of the LM8 sublines: their expression levels were high in LM8-H cells and low in LM8-L and LM8-H/*Lef1*-KO cells. Their expression levels were confirmed by qualitative PCR (qPCR) (Figure 4B; Figure S6). Protein-expression level of CYGB was

sufficiently correlated with the metastatic phenotype of LM8 sublines: CYGB was highly expressed in LM8-H cells but not in LM8-L and LM8-H/*Lef1*-KO cells (Figure 4C). For subsequent studies, we analyzed *Cygb* because the function of *Cygb* in metastasis has not yet been described, whereas *Ddx58* has been reported to promote lung metastasis in several types of cancer.^{36,37}

3.5 | Function of CYGB in the extravasation of LM8 sublines

To assess the correlation between CYGB-expression level and extravasation ability of the LM8 sublines, we established stable cell clones, including a CYGB-overexpressing LM8-L (LM8-L/CYGB-OE) clone and 2 independent *Cygb*-KO LM8-H (LM8-H/*Cygb*-KO1 and LM8-H/*Cygb*-KO2) clones using 2 gRNAs (Figure 5A). KO of *Cygb* increased the cell-proliferation rate compared to LM8-H cells and CYGB-OE decreased it (Figure 5B). These results are consistent with our results showing that *Lef1*-KO cells increased the proliferation rate of LM8-H cells (Figure S2), suggesting that CYGB is a downstream effector of LEF1. Adhesion and transmigration abilities were significantly higher in LM8-L/CYGB-OE cells compared to LM8-L cells (Figure 5C). In contrast, KO of *Cygb* significantly decreased the

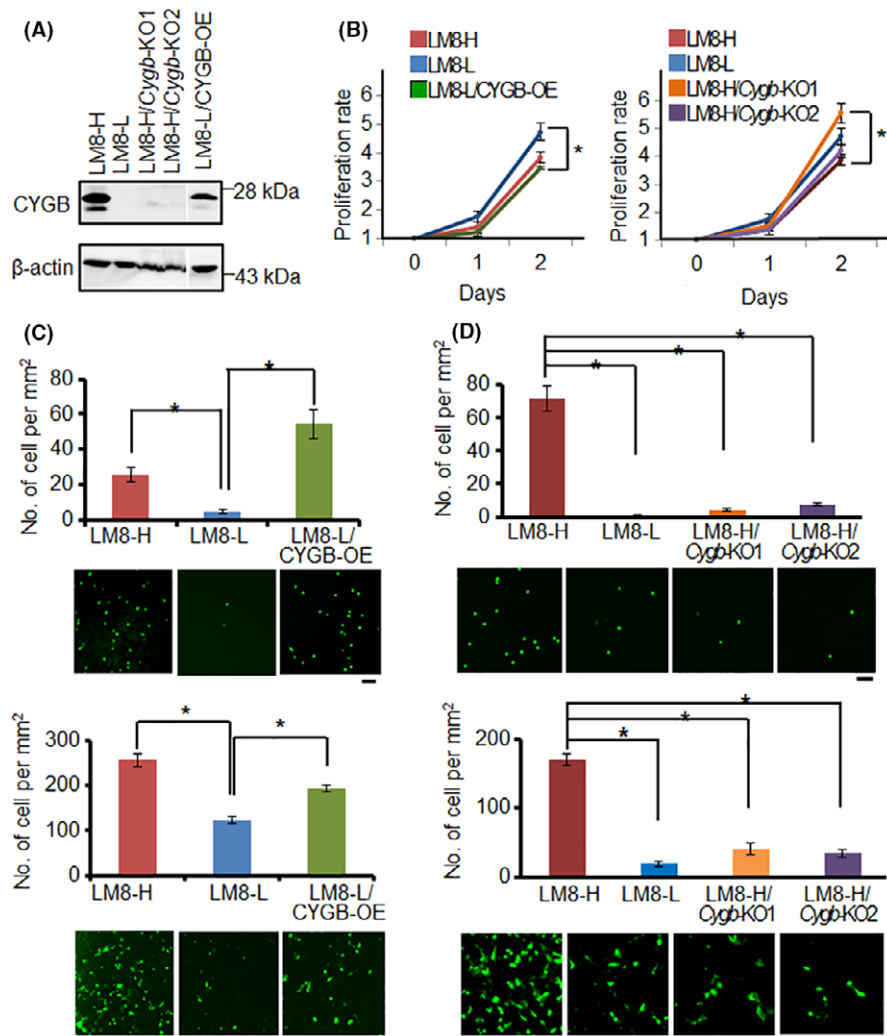


FIGURE 5 Function of CYGB in the extravasation of LM8 sublines. A, Protein-expression levels of CYGB in LM8-H/*Cygb*-KO and LM8-L/CYGB-OE cells. B, Cell-proliferation rates of the LM8 sublines. C, D, Ability of the LM8 sublines to adhere to and transmigrate to the vascular endothelial monolayer. Adhesion and transmigration abilities of LM8-L/CYGB-OE (C) and LM8-H/*Cygb*-KO (D) cells were quantitatively analyzed (graphs) by determining the number of fluorescently labeled cells attached to (upper) and transmigrating through (lower) a vascular endothelial monolayer, respectively. Representative images are shown depicting the fluorescently labeled cells that were counted (photos). $n = 3$, $*P < .05$. Bars, 100 μm . CYGB, cytoglobin

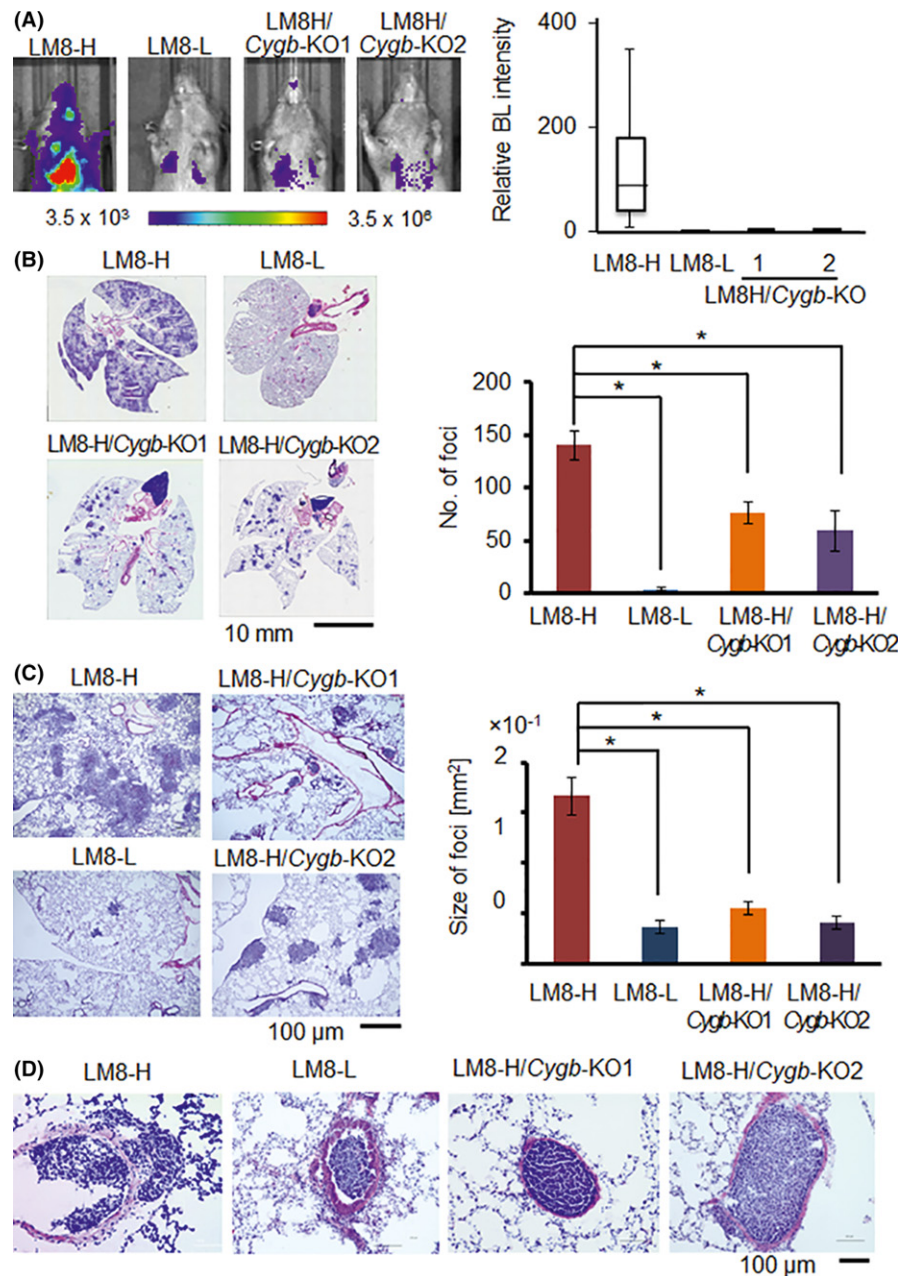


FIGURE 6 Knockout of *Cygb* suppressed the lung-metastatic ability of LM8-H cells in vivo. A, Bioluminescence (BL) images of mice injected with the indicated cells on day 16. Relative BL signals to day 0 are shown in the right box plot. B, Representative HE staining of the lung at 16 days after i.v. injection of LM8 sublines (left). Number of foci in the lung on day 16 (right). $n = 4$ * $P < .05$. C, Representative HE-stained lung (left) and size of foci in the lung (right) at 16 days after i.v. injection. $n = 32$ * $P < .05$. D, Enlarged representative images of metastatic foci of the LM8 sublines on day 16. *Cygb*, cytoglobin gene

adhesion and transmigration abilities of LM8-H cells (Figure 5D). These results strongly suggest that CYGB promoted extravasation with the LM8 sublines by increasing their adhesion and transmigration abilities.

3.6 | Knockout of *Cygb* suppressed the lung-metastatic ability of LM8-H cells in vivo

To assess the function of CYGB in lung extravasation, the metastatic ability of *Cygb*-KO LM8-H (LM8-H/*Cygb*-KO) cells was examined in vivo. LM8 sublines were i.v. injected into C3H mice and BL signals in the lungs were monitored for 16 days. Strikingly, LM8-H/*Cygb*-KO cells showed significantly decreased lung metastasis compared to LM8-H cells (Figure 6A). HE staining of the lungs from mice 16 days after injection of the LM8 sublines confirmed the regulatory function

of CYGB in lung metastasis: KO of *Cygb* in LM8-H cells significantly reduced the number of lung-metastatic foci (Figure 6B). The size of foci in the lungs was significantly smaller in the LM8-H/*Cygb*-KO group compared to the LM8-H group (Figure 6C). LM8-H/*Cygb*-KO cells failed to extravasate into the lung parenchyma and remained and grew in the lung blood vessels (Figure 6D; Figure S3). Together, these results support the function of CYGB in extravasation in lung metastasis of the LM8 sublines.

4 | DISCUSSION

In the present study, we identified CYGB as an important regulator of OS extravasation and highlighted the importance of the LEF1-CYGB regulatory axis in OS metastasis to the lungs. To our

knowledge, this is the first report showing a functional connection between LEF1 and CYGB.

To explore the possibility that LEF1 directly regulates the expression of CYGB, genome analysis of transcription factor binding sites was carried out using several databases³⁸⁻⁴² and showed that *Cygb* has potential LEF1 binding sites in the promoter region (Figure S7). LEF1 may directly regulate *Cygb* expression. As CYGB is known to be induced by HIF-1 α , NF- κ B, and other inflammation-related transcription factors,²³ the interaction of LEF1 with these transcription factors may be important for regulating *Cygb* expression. Among the 737 genes that were differentially expressed between LM8-L and LM8-H cells, 21 genes were selected as candidate genes responsible for lung metastasis of LM8-H by genomewide meta-analysis, using public data sets from patients with high- and low-metastatic OS. Expression of 13 out of 21 genes correlated well with cancer prognosis in patients with OS (Figure S4). The gene products of the 13 selected genes function as cell receptors/transporters, cytokines, GTPase-activating proteins and in cell movement (Table S3) and most of the candidate genes have previously been associated with malignant progression. *Cygb* is defined as a tumor suppressor gene, and its expression is suppressed by the methylation of nucleotides in the promoter region of many types of cancer.¹⁹ To our knowledge, the function of CYGB in metastasis, especially extravasation and cell-cell interactions in cancer, has not yet been reported.

The KO of *Cygb* in LM8-H cells clearly demonstrated the significance of CYGB in lung metastasis. The number and size of metastatic foci in LM8-H/*Cygb*-KO cells were strongly suppressed, even though the proliferation rate of LM8-H/*Cygb*-KO cells was higher than that of LM8-H cells (Figure 5B). Moreover, LM8-L and LM8-H/*Cygb*-KO cells showed a higher frequency of remaining in pulmonary blood vessels than LM8-H (Figure S7), supporting lower extravasation ability of these cells. However, the number of metastatic foci of LM8-H/*Cygb*-KO cells was higher than that of LM8-L cells, suggesting that other downstream effectors of LEF1 also contribute to the lung-metastatic phenotype of LM8-H cells. Furthermore, the ability of adhesion and transmigration (Figure 3B,C) and the level of *Cygb* expression (Figure 4B) were higher in LM8-H/*Lef1*-KO1 cells than in LM8-L cells. These results suggest that the expression of *Cygb* could also be regulated by a LEF1-independent mechanism.

We conducted 2 experiments to elucidate the molecular mechanism by which CYGB functions directly in promoting extravasation based on the proposed functions for CYGB. First, as CYGB has been suggested to act as an NO dioxygenase⁴³ and as NO prevents endothelial activation by inhibiting the expression of adhesion molecules such as vascular cell adhesion molecule 1 (VCAM-1) and intercellular adhesion molecule 1 (ICAM-1),^{44,45} we investigated whether CYGB reduces NO levels in the lung blood vessels, in turn, reducing the expression of adhesion molecules. We found only slight differences in the total NO species levels and little influence of inhibitors of NO species among the LM8 sublines (Figure S9). Although NO reduction by CYGB may

contribute to metastasis, the subtle differences in NO levels among the LM8 sublines cannot explain the significant differences in lung-metastatic potential found among them, suggesting that NO is not a major player in CYGB-mediated extravasation. Second, as arachidonic acid (AA) increases the migratory activity of cancer cells through activation of RhoA and RhoC,⁴⁶ and as recent findings imply that CYGB functions in lipid oxidation,⁴⁷ thereby modifying several types of phospholipids such as phosphatidylinositol (3,4,5)-trisphosphate (an important signal mediator of the AKT signaling pathway) to form arachidonoyl-containing lipid, we examined the content of AA in the LM8 sublines. No difference was found in the AA contents among the LM8 sublines (Figure S10), suggesting that AA did not function as an effector molecule of CYGB to promote lung metastasis in the LM8 sublines. These results suggest that the function of CYGB which has not yet been identified contributes to promotion of the extravasation.

As we used an i.v. injection model to examine the lung-metastatic abilities of the LM8 sublines, our evaluation was limited to the postcirculation steps of metastasis. To explore the differences between LM8-H and LM8-L cells in precirculation steps, we analyzed the EMT and invasion steps. Although the morphologies of LM8-H and LM8-L cells differ, the expression levels of EMT-related genes (based on microarray data) and the migration and invasion abilities (assessed by wound-healing and invasion assays, respectively) were not significantly different between either cell line (Table S4; Figure S11). These findings suggest that their metastatic abilities may not be so very different before the intravasation steps. Because in vitro analyses using cell-adhesion and transmigration assays can also assess their intravasation capacities, the results suggest that LM8-L also has low intravasation ability. Therefore, LM8-L cells may further reduce the frequency of metastasis from the primary tumor site to the lungs when assessed in a model of the total metastasis process. Further studies elucidating the entire LEF1-CYGB axis should contribute to the development of new therapeutic approaches for preventing OS metastasis to the lungs.

ACKNOWLEDGMENTS

We thank Biomaterials Analysis Division, Technical Department of Tokyo Institute of Technology for technical support. We also thank Shimadzu Corporation for technical support of AA analysis with LC/MS in Shimadzu corporation precision analytical instruments room of Tokyo Institute of Technology.

CONFLICTS OF INTEREST

Authors declare no conflicts of interest for this article.

ORCID

Shinae Kizaka-Kondoh  <http://orcid.org/0000-0003-3085-5782>

REFERENCES

1. Savage S, Mirabello L. Using epidemiology and genomics to understand osteosarcoma etiology. *Sarcoma*. 2011;2011:1-13.
2. Yang G, Yuan J, Li K. EMT transcription factors: implication in osteosarcoma. *Med Oncol*. 2013;30:1-5.
3. Aljbran AH, Griffin A, Pintilie M, et al. Osteosarcoma in adolescents and adults: survival analysis with and without lung metastases. *Ann Oncol*. 2009;20:1136-1141.
4. Isakoff MS, Bielack SS, Meltzer P, et al. Osteosarcoma: current treatment and a collaborative pathway to success. *J Clin Oncol*. 2015;33:3029-3035.
5. Hunter KW, Crawford NPS, Alsarraj J. Mechanisms of metastasis. *Breast Cancer Res*. 2008;10(Suppl 1):S2.
6. Lambert AW, Pattabiraman DR, Weinberg RA. Emerging biological principles of metastasis. *Cell*. 2017;168:670-691.
7. Strilic B, Offermanns S. Intravascular survival and extravasation of tumor cells. *Cancer Cell*. 2017;32:282-293.
8. Reymond N, D'Agua BB, Ridley AJ. Crossing the endothelial barrier during metastasis. *Nat Rev Cancer*. 2013;13:858-870.
9. Liu Y, Wang W, Xu J, et al. Dihydroartemisinin inhibits tumor growth of human osteosarcoma cells by suppressing Wnt/ β -catenin signaling. *Oncol Rep*. 2013;30:1723-1730.
10. Xu M, Jin H, Xu C-XX, et al. MiR-34c inhibits osteosarcoma metastasis and chemoresistance. *Med Oncol*. 2014;31:972-979.
11. Santiago L, Daniels G, Wang D, et al. Wnt signaling pathway protein LEF1 in cancer, as a biomarker for prognosis and a target for treatment. *Am J Cancer Res*. 2017;7:1389-1406.
12. Eastman Q, Grosschedl R. Regulation of LEF-1/TCF transcription factors by Wnt and other signals. *Curr Opin Cell Biol*. 1999;11:233-240.
13. Burmester T, Ebner B, Weich B, et al. Cytoglobin: a novel globin type ubiquitously expressed in vertebrate tissues. *Mol Biol Evol*. 2002;19:416-421.
14. Burmester T, Haberkamp M, Mitz S, et al. Neuroglobin and cytoglobin: genes, proteins and evolution. *IUBMB Life*. 2004;56:703-707.
15. Kawada N, Kristensen DB, Asahina K, et al. Characterization of a stellate cell activation-associated protein (STAP) with peroxidase activity found in rat hepatic stellate cells. *J Biol Chem*. 2001;276:25318-25323.
16. John R, Chand V, Chakraborty S, et al. DNA damage induced activation of Cygb stabilizes p53 and mediates G1 arrest. *DNA Repair (Amst)*. 2014;24:107-112.
17. Xu H-W, Huang Y-J, Xie Z-Y, et al. The expression of cytoglobin as a prognostic factor in gliomas: a retrospective analysis of 88 patients. *BMC Cancer*. 2013;13:1-9.
18. Thuy LTT, Matsumoto Y, Van Thuy TT, et al. Cytoglobin deficiency promotes liver cancer development from hepatosteatosis through activation of the oxidative stress pathway. *Am J Pathol*. 2015;185:1045-1060.
19. Oleksiewicz U, Liloglou T, Tasopoulou K-M, et al. Cytoglobin has bimodal: tumour suppressor and oncogene functions in lung cancer cell lines. *Hum Mol Genet*. 2013;22:3207-3217.
20. Yu X, Gao D. Overexpression of cytoglobin gene inhibits hypoxic injury to SH-SY5Y neuroblastoma cells. *Neural Regen Res*. 2013;8:2198-2203.
21. Tian S-F, Yang H-H, Xiao D-P, et al. Mechanisms of neuroprotection from hypoxia-ischemia (HI) brain injury by up-regulation of cytoglobin (CYGB) in a neonatal rat model. *J Biol Chem*. 2013;288:15988-16003.
22. Tanaka F, Tominaga K, Sasaki E, et al. Cytoglobin may be involved in the healing process of gastric mucosal injuries in the late phase without angiogenesis. *Dig Dis Sci*. 2013;58:1198-1206.
23. Fordel E, Geuens E, Dewilde S, et al. Hypoxia/Ischemia and the regulation of neuroglobin and cytoglobin expression. *IUBMB Life*. 2004;56:681-687.
24. Asai T, Ueda T, Itoh K, et al. Establishment and characterization of a murine osteosarcoma cell line (LM8) with high metastatic potential to the lung. *Int J Cancer*. 1998;76:418-422.
25. Kuchimaru T, Hoshino T, Aikawa T, et al. Bone resorption facilitates osteoblastic bone metastatic colonization by cooperation of insulin-like growth factor and hypoxia. *Cancer Sci*. 2014;105:553-559.
26. Abràmoff MD, Magalhães PJ, Ram SJ. Image processing with ImageJ. *Biophotonics Int*. 2004;11:36-41.
27. Smedley D, Haider S, Durinck S, et al. The BioMart community portal: an innovative alternative to large, centralized data repositories. *Nucleic Acids Res*. 2015;43:W589-W598.
28. Ran FA, Hsu PD, Wright J, et al. Genome engineering using the CRISPR-Cas9 system. *Nat Protoc*. 2013;8:2281-2308.
29. Mashiko D, Young SAM, Muto M, et al. Feasibility for a large scale mouse mutagenesis by injecting CRISPR/Cas plasmid into zygotes. *Dev Growth Differ*. 2014;56:122-129.
30. Cui Z, Geurts AM, Liu G, et al. Structure-function analysis of the inverted terminal repeats of the sleeping beauty transposon. *J Mol Biol*. 2002;318:1221-1235.
31. Aronovich EL, Mclvor RS, Hackett PB. The sleeping beauty transposon system: a non-viral vector for gene therapy. *Hum Mol Genet*. 2011;20:R14-R20.
32. Ivics Z, Hackett PB, Plasterk RH, et al. Molecular reconstruction of sleeping beauty, a tc1-like transposon from fish, and its transposition in human cells. *Cell*. 1997;91:501-510.
33. Dräger J, Simon-Keller K, Pukrop T, et al. LEF1 reduces tumor progression and induces myodifferentiation in a subset of rhabdomyosarcoma. *Oncotarget*. 2017;8:3259-3273.
34. Gutierrez A, Sanda T, Ma W, et al. Inactivation of LEF1 in T-cell acute lymphoblastic leukemia. *Blood*. 2010;115:2845-2851.
35. Goswami C, Nakshatri H. PROGgeneV2: enhancements on the existing database. *BMC Cancer*. 2014;14:970-975.
36. Chang Y-C, Chi L-H, Chang W-M, et al. Glucose transporter 4 promotes head and neck squamous cell carcinoma metastasis through the TRIM24-DDX58 axis. *J Hematol Oncol*. 2017;10:1-12.
37. Ghildiyal R, Sen E. CK2 induced RIG-I drives metabolic adaptations in IFN γ -treated glioma cells. *Cytokine*. 2017;89:219-228.
38. Kreft L, Soete A, Hulpiau P, et al. ConTra v3: a tool to identify transcription factor binding sites across species, update 2017. *Nucleic Acids Res*. 2017;45:W490-W494.
39. Matys V, Kel-Margoulis OV, Fricke E, et al. TRANSFAC[®] and its module TRANSCompel[®]: transcriptional gene regulation in eukaryotes. *Nucleic Acids Res*. 2006;34:D108-D110.
40. Portales-Casamar E, Thongjuea S, Kwon AT, et al. JASPAR 2010: the greatly expanded open-access database of transcription factor binding profiles. *Nucleic Acids Res*. 2010;38:D105-D110.
41. Weirauch MT, Yang A, Albu M, et al. Determination and inference of eukaryotic transcription factor sequence specificity. *Cell*. 2014;158:1431-1443.
42. Jolma A, Yan J, Whittington T, et al. DNA-binding specificities of human transcription factors. *Cell*. 2018;152:327-339.
43. Gardner AM, Cook MR, Gardner PR. Nitric-oxide dioxygenase function of human cytoglobin with cellular reductants and in rat hepatocytes. *J Biol Chem*. 2010;285:23850-23857.
44. Khan BV, Harrison DG, Olbrych MT, et al. Nitric oxide regulates vascular cell adhesion molecule 1 gene expression and redox-sensitive transcriptional events in human vascular endothelial cells. *Proc Natl Acad Sci USA*. 1996;93:9114-9119.
45. De Caterina R, Libby P, Peng HB, et al. Nitric oxide decreases cytokine-induced endothelial activation. Nitric oxide selectively reduces

- endothelial expression of adhesion molecules and proinflammatory cytokines. *J Clin Invest*. 1995;96:60-68.
46. Brown M, Roulson J-A, Hart CA, et al. Arachidonic acid induction of Rho-mediated transendothelial migration in prostate cancer. *Br J Cancer*. 2014;110:2099-2108.
47. Tejero J, Kapralov AA, Baumgartner MP, et al. Peroxidase activation of cytoglobin by anionic phospholipids: mechanisms and consequences. *Biochim Biophys Acta*. 2016;1861:391-401.

How to cite this article: Pongsuchart M, Kuchimaru T, Yonezawa S, et al. Novel lymphoid enhancer-binding factor 1-cytoglobin axis promotes extravasation of osteosarcoma cells into the lungs. *Cancer Sci*. 2018;109:2746–2756.
<https://doi.org/10.1111/cas.13702>

SUPPORTING INFORMATION

Additional supporting information may be found online in the Supporting Information section at the end of the article.